*Journal of Statistical Physics, Vol. 11, No. 1, 1974*

# Statistical Mechanics of Zero-Dimensional Ginzburg-Landau Fields: Accuracy of the Screening Approximation

Alan J. Bray[1]

*Received March 12, 1974*

The screening approximation of Ferrell and Scalapino ($n^{-1}$ expansion) is tested in the exactly soluble zero-dimensional case. The expansion is carried to fifth order in $n^{-1}$, where, for $n = 2$, it appears to start diverging. For $n = 1$ divergence sets in at the second-order term. The "self-consistent" screening approximation of Bray and Rickayzen converges more rapidly but is more difficult to apply in higher dimensionalities. The usefulness of the zero-dimensional case for checking the enumeration of the Feynman graphs which appear in third and higher order is emphasized.

**KEY WORDS:** Ginzburg–Landau model; entropy function; $1/n$ expansion; screening.

## 1. INTRODUCTION

A recent approach[1–4] to the theory of the critical behavior of the $d$-dimensional Ginzburg–Landau model with $n$ components of the order parameter has been based on providing systematic corrections to the Hartree approximation by means of an expansion in powers of $1/n$. This has been termed the "screening approximation" since its graph-theoretic derivation

[1] Center for Theoretical Physics, Department of Physics and Astronomy, University of Maryland, College Park, Maryland.

involves graphs in which the bare interaction between fluctuations of the order parameter field is screened by the insertion of polarization loops. Applications have been made to the cases $d = 1$[4] (to second order in $1/n$) and $d = 2, 3$[1,3] (both to first order in $1/n$). Here the expansion in powers of $1/n$ refers to the calculation of a thermodynamic function (typically the specific heat) per component of the order parameter. For the specific heat per component we have $C = C_0 + (1/n)C_1 + (1/n^2)C_2 + \cdots$, where $C_0$ follows from the Hartree approximation. For $d = 1$ the expansion may be performed either graphically[5] or nongraphically[4] but for $d = 2$ or 3 no nongraphical methods are known as yet.

The present work is concerned with a detailed test of the screening approximation for the especially simple case $d = 0$, which corresponds to a situation in which there are no spatial fluctuations of the order parameter field. The $1/n$ expansion is carried to fifth order and compared with exact results for $n = 2$ and $n = 1$. For $n = 2$ we find that the accuracy of the approximation improves through third- and fourth-order corrections and then seems to start deteriorating when the fifth-order correction is included. For $n = 1$ divergence sets in as early as the second-order screening correction. Also tested here is the "self-consistent" screening approximation of Bray and Rickayzen.[6,7] This was originally introduced[6] as a graph-theoretic interpolation between Hartree and Hartree–Fock approximations in order to reproduce correct behavior in both high- and low-temperature regimes. It is shown here to correspond to an iteration of the coupled equations for the self-energy and three-point vertex using the Hartree approximation as starting point. For $d = 0$ we find that this self-consistent scheme converges more rapidly than the simple $1/n$ expansion. It is, however, more difficult to extend to the cases $d = 1$, 2, and 3.

In Section 2 we introduce the model and its well-known exact solutions for $d = 0$. As for the case $d = 1$, there is no sharp phase transition for this case.[2] Section 3 is devoted to a discussion of the $1/n$ expansion for $d = 0$. We find it convenient to derive a first-order (nonlinear) differential equation satisfied by the entropy. The form of this equation renders the expansion in powers of $1/n$ straightforward, the case $n = \infty$ reducing to the usual Hartree limit. Section 4 deals with the self-consistent screening approximation. Instead of expanding in powers of $1/n$, an iteration of the differential equation derived previously, using the Hartree result as starting point, produces results which converge more rapidly. In Section 5 we consider the problem from the graph-theoretic viewpoint. Use of the familiar Ward identity relating the derivative of the self-energy to the three-point vertex enables us to sum all graphs for the propagator of the order parameter field. The result is a re-

[2] This is no longer true for $n < 0$ ($d = 0$) and $n < 1$ ($d = 1$).[8]

covery of the differential equation derived in Section 3. Graphs for the first- and second-order screening corrections to the entropy are written down and used to recover the results of Section 3. A discussion of the graphs for the free energy is contained in Section 6. The advantage of the graph-theoretic approach is that it is amenable in principle to an extension to higher dimensionalities, but we do not attempt this here. Section 7 concludes with a brief summary.

## 2. THE MODEL AND ITS SOLUTIONS

The Ginzburg–Landau model in $d$ dimensions is defined by the following partition function:

$$Z = \int \prod_{i=1}^{n} [d\phi_i(x)] \exp\{-F[\phi_i(x)]\} \tag{1}$$

where the free energy functional $F$ is given by the canonical form

$$F[\phi_i(x)] = \int d^d x \left\{ \frac{1}{2} \sum_{i=1}^{n} [\tau \phi_i^2 + (\nabla \phi_i)^2] + \frac{1}{4n} \left( \sum_{i=1}^{n} \phi_i^2 \right)^2 \right\} \tag{2}$$

and $\phi_i(x)$, $i = 1,\ldots, n$, is an $n$-component order parameter field. The presence of the explicit $1/n$ in the coefficient of the fourth-order term of Eq. (2) ensures that the width of the critical region is independent of $n$ in the Hartree limit ($n \to \infty$) and thereby makes possible the expansion in powers of $1/n$.

In the special case $d = 0$ there are no spatial fluctuations of the order parameter and the partition function reduces to an integral over the magnitude of the $\phi_i$:

$$Z = \int_{-\infty}^{\infty} \prod_i d\phi_i \exp\left[ -\tfrac{1}{2}\tau \sum \phi_i^2 - (1/4n) \left( \sum \phi_i^2 \right)^2 \right] \tag{3}$$

Equation (3), with $n = 2$, has been used as a model for the thermodynamics of small, superconducting grains[9] of diameter less than 1000 Å (but not so small that the discrete nature of the electronic energy spectrum becomes important.) It may be simplified by the substitution $\sum_i \phi_i^2 = \phi^2$ to yield

$$Z = C_n \int_0^{\infty} \phi^{n-1}\, d\phi \exp[-\tfrac{1}{2}\tau\phi^2 - (1/4n)\phi^4] \tag{4}$$

where $C_n = 2\pi^{n/2}/\Gamma(n/2)$ is the area of the unit hypersphere in $n$ dimensions.

A change of integration variable to $S = (2n)^{-1/2}\phi^2$ yields

$$Z = \frac{1}{2} C_n (2n)^{n/4} \int_0^\infty dS\, S^{n/2-1} \exp\left[-\left(\frac{n}{2}\right)^{1/2} \tau S - \frac{1}{2} S^2\right]$$

$$= (2\pi^2 n)^{n/4} \left(\exp \frac{n\tau^2}{8}\right) U\left(\frac{n-1}{2}, \left(\frac{n}{2}\right)^{1/2} \tau\right), \qquad \tau > 0 \tag{5}$$

$$= (2\pi^2 n)^{n/4} \left(\exp \frac{n\tau^2}{8}\right) \left\{ \frac{\pi}{\Gamma(n/2)} V\left(\frac{n-1}{2}, -\left(\frac{n}{2}\right)^{1/2} \tau\right) \right.$$

$$\left. - \sin\left[(n-1)\frac{\pi}{2}\right] U\left(\frac{n-1}{2}, -\left(\frac{n}{2}\right)^{1/2} \tau\right) \right\}, \qquad \tau < 0 \tag{6}$$

where $U(a, x)$ and $V(a, x)$ are the parabolic cylinder functions.[10]

For the purposes of the $1/n$ expansion it will be convenient to define an entropy function by $\theta = -(2/n)\, d(\ln Z)/d\tau$ ($\theta$ is minus twice the entropy per component of the order parameter). $\theta$ may be calculated either by differentiating Eq. (6) directly and using the recursions relations[10] for $U$ and $V$, or by differentiating inside the integral of Eq. (4). The latter technique gives

$$\theta = \frac{1}{n} \frac{\int_0^\infty \phi^{n+1}\, d\phi \exp[-\frac{1}{2}\tau\phi^2 - (1/4n)\phi^4]}{\int_0^\infty \phi^{n-1}\, d\phi \exp[-\frac{1}{2}\tau\phi^2 - (1/4n)\phi^4]} \tag{7}$$

$$= \left(\frac{2}{n}\right)^{1/2} \frac{\int_0^\infty S^{n/2}\, dS \exp[-\tau(\frac{1}{2}n)^{1/2} S - \frac{1}{2}S^2]}{\int_0^\infty S^{n/2-1}\, dS \exp[-\tau(\frac{1}{2}n)^{1/2} S - \frac{1}{2}S^2]}$$

$$= \left(\frac{n}{2}\right)^{1/2} \frac{U(\frac{1}{2}(n+1), \tau(\frac{1}{2}n)^{1/2})}{U(\frac{1}{2}(n-1), \tau(\frac{1}{2}n)^{1/2})}, \qquad \tau > 0$$

$$= \left(\frac{n}{2}\right)^{1/2} \frac{\pi}{\Gamma(\frac{1}{2}n+1)} \left\{ V\left(\frac{n+1}{2}, -\tau\left(\frac{n}{2}\right)^{1/2}\right) \right.$$

$$\left. - \sin\left[(n+1)\frac{\pi}{2}\right] U\left(\frac{n+1}{2}, -\tau\left(\frac{n}{2}\right)^{1/2}\right) \right\}$$

$$\times \left\{ \frac{\pi}{\Gamma(\frac{1}{2}n)} V\left(\frac{n-1}{2}, -\tau\left(\frac{n}{2}\right)^{1/2}\right) - \sin\left[(n-1)\frac{\pi}{2}\right] \right.$$

$$\left. \times\, U\left(\frac{n-1}{2}, -\tau\left(\frac{n}{2}\right)^{1/2}\right) \right\}^{-1}, \qquad \tau < 0 \tag{8}$$

For $n = 2$ the result takes a particularly simple form. Returning to Eq. (4) and setting $n = 2$ yields

$$Z(n=2) = C_2 \int_0^\infty \phi\, d\phi \exp(-\tfrac{1}{2}\tau\phi^2 - \tfrac{1}{8}\phi^4)$$

A change of integration variable to $t = \phi^2/2\sqrt{2}$ gives

$$\begin{aligned} Z(n=2) &= \sqrt{2}C_2 \int_0^\infty dt \exp(-\sqrt{2}\tau t - t^2) \\ &= \sqrt{2}C_2[\exp(\tau^2/2)] \int_{\tau/\sqrt{2}}^\infty dt \exp(-t^2) \\ &= (\pi/2)^{1/2} C_2 \exp(\tau^2/2) \operatorname{erfc}(\tau/\sqrt{2}) \end{aligned} \tag{9}$$

The entropy function becomes

$$\theta(n=2) = -\tau + (2/\pi)^{1/2} \exp(-\tau^2/2)/\operatorname{erfc}(\tau/\sqrt{2}) \tag{10}$$

Equations (9) and (10) are the well-known results for the $d = 0$ superconductor. Plots of $\theta$ versus $\tau$ for $n = 2$ and $n = 1$ are given in Figs. 1 and 3.

## 3. THE $1/n$ EXPANSION FOR $d = 0$

The $1/n$ expansion was originally conceived[1,2] as a Feynman graph expansion in which the order (in $1/n$) of a graph is equal to the difference between the number of interaction vertices and the number of closed loops. This is the form of the expansion which has been used[1,3] to calculate leading corrections to the Hartree results in $d = 3$ and $d = 2$. Since, however, the number of graphs rapidly increases with the order in $1/n$, nongraphical techniques, where they exist, are in many ways preferable. Such a technique, based on solving the equivalent quantum mechanical anharmonic oscillator problem,[11] has been used by Ferrell and Scalapino[4] to calculate the first two screening corrections for $d = 1$.

The simplest way of dealing with the $1/n$ expansion for $d = 0$ is by means of a differential equation for the entropy function $\theta$. Recall the definition of $\theta$:

$$\theta = -\frac{2}{n}\frac{d \ln Z}{d\tau} = -\frac{2}{n}\frac{1}{Z}\frac{dZ}{d\tau}$$

Hence

$$\begin{aligned} \frac{d\theta}{d\tau} &= -\frac{2}{n}\frac{1}{Z}\frac{d^2Z}{d\tau^2} + \frac{2}{n}\left(\frac{1}{Z}\frac{dZ}{d\tau}\right)^2 \\ &= -\frac{2}{n}\frac{1}{Z}\frac{d^2Z}{d\tau^2} + \frac{n}{2}\theta^2 \end{aligned}$$

The first term on the right-hand side is evaluated by differentiating inside the integral of Eq. (4) to give

$$\frac{1}{Z}\frac{d^2Z}{d\tau^2} = \frac{1}{4}\frac{\int_0^\infty \phi^{n+3}\, d\phi \exp[-\frac{1}{2}\tau\phi^2 - (1/4n)\phi^4]}{\int_0^\infty \phi^{n-1}\, d\phi \exp[-\frac{1}{2}\tau\phi^2 - (1/4n)\phi^4]}$$

Integration of the numerator by parts yields, recalling that $\theta$ satisfies Eq. (7),

$$\frac{1}{Z}\frac{d^2Z}{d\tau^2} = \frac{n^2}{4}(1 - \tau\theta)$$

giving

$$\frac{d\theta}{d\tau} = \frac{n}{2}\theta^2 - \frac{n}{2}(1 - \tau\theta)$$

or

$$\theta^2 + \tau\theta = 1 + \frac{2}{n}\frac{d\theta}{d\tau} \tag{11}$$

Equation (11) is a nonlinear first-order differential equation for $\theta$. Being of the Ricatti type, it may be transformed to a linear second-order differential equation for $Z$, where $\theta = -(2/n)(1/Z)\, dZ/d\tau$, which not unnaturally turns out to be the generating equation for the parabolic cylinder functions $U$ and $V$. In its present form, however, Eq. (11) is eminently suited to an expansion in powers of $1/n$. Setting $n = \infty$ removes the first derivative term to give the usual Hartree limit:

$$\theta_0^2 + \tau\theta_0 = 1 \tag{12}$$

or

$$\theta_0 = [(\tau^2 + 4)^{1/2} - \tau]/2 \tag{13}$$

This result is independent of $n$. It is compared to the exact results for $n = 2$ and $n = 1$ in Figs. 1 and 3. Not unexpectedly, the Hartree result is a rather poor approximation for these small values of $n$. Before continuing with the $1/n$ expansion, we state the boundary condition needed to specify a unique solution of Eq. (11). This is clearly $\theta \to 1/\tau$ as $\tau \to +\infty$ since this result follows directly from Eq. (7), the $\phi^4$ terms being negligible in the limit of large, positive $\tau$. The Hartree result already satisfies this boundary condition and it is clear from Eq. (11) that all corrections to the Hartree result will vanish more quickly than $1/\tau$ as $\tau \to +\infty$. Hence when we make the $1/n$ expansion the boundary condition is satisfied ab initio.

We now proceed with the $1/n$ expansion. We will find it convenient to set $\lambda = 2/n$ and look for the expansion in powers of $\lambda$. Setting

$$\theta(\tau) = \sum_{r=0}^{\infty} \theta_r(\tau)\lambda^r$$

in Eq. (11) yields

$$\sum_{r,s=0}^{\infty} \theta_r\theta_S\lambda^{r+S} + \tau\sum_{r=0}^{\infty} \theta_r\lambda^r = 1 + \sum_{r=0}^{\infty} (d\theta_r/d\tau)\lambda^{r+1}$$

Equating coefficients of $\lambda^0$ gives the Hartree result, Eq. (12). Equating coefficients of $\lambda^r$ for $r \geqslant 1$ yields

$$\sum_{S=0}^{r} \theta_S \theta_{r-S} + \tau\theta_r = d\theta_{r-1}/d\tau$$

Terms involving $\theta_r$ may be extracted from the sum to give

$$\sum_{S=1}^{r-1} \theta_S \theta_{r-S} + (2\theta_0 + \tau)\theta_r = d\theta_{r-1}/d\tau$$

or

$$\theta_r = \frac{-\theta_0}{1 + \theta_0^2}\left(\frac{\theta_0^2}{1 + \theta_0^2}\frac{d\theta_{r-1}}{d\theta_0} + \sum_{S=1}^{r-1} \theta_S \theta_{r-S}\right) \tag{14}$$

where we have used Eq. (12) to eliminate $\tau$ in favor of $\theta_0$. Equation (14) yields the following expressions for $\theta_r$ for $r = 1$–5:

$$\begin{aligned}
\theta_1 &= -\theta_0^3/(1 + \theta_0^2)^2 \\
\theta_2 &= \theta_0^5(3 - 2\theta_0^2)/(1 + \theta_0^2)^5 \\
\theta_3 &= -5\theta_0^7(3 - 7\theta_0^2 + 2\theta_0^4)/(1 + \theta_0^2)^8 \\
\theta_4 &= \theta_0^9(105 - 489\theta_0^2 + 437\theta_0^4 - 74\theta_0^6)/(1 + \theta_0^2)^{11} \\
\theta_5 &= -\theta_0^{11}(945 - 7044\theta_0^2 + 12{,}308\theta_0^4 - 6117\theta_0^6 + 706\theta_0^8) \\
&\quad \times (1 + \theta_0^2)^{-14}
\end{aligned} \tag{15}$$

Successive screening approximations are generated by the formula

$$\theta(n = 2/\lambda) = \sum_{r=0}^{k} \theta_r \lambda^r, \qquad k = 0, 1, 2,... \tag{16}$$

We shall refer to Eq. (16) as the "$k$th screening approximation." We consider first the case $n = 2$ ($\lambda = 1$). Exact, Hartree, and first screening solutions are shown in Fig. 1. Higher screening approximations are so accurate that we depict them in terms of their differences from the exact result. These differences, $\theta - \sum_{r=0}^{k} \theta_r \lambda^r$, are plotted versus $\tau/\sqrt{2}$ for $k = 1$–5 in Fig. 2. Note that the accuracy of the approximation improves through $k = 3$ or 4 and then seems to start deteriorating for $k = 5$. This may be symptomatic of the asymptotic nature of the $1/n$ expansion. That the $1/n$ expansion cannot be convergent is easily demonstrated by considering the point $\tau = 0$. For this special case the integrals in Eq. (7) are readily evaluated to yield

$$\theta(n, \tau = 0) = (2/\sqrt{n})\Gamma(n/4 + \tfrac{1}{2})/\Gamma(n/4)$$

This function has poles at $n = -2, -6, -10,...$, so that considered as a function of $1/n$, it can have no finite radius of convergence. In fact the usual expansion of the gamma functions for large $n$ shows that the expansion in powers of $1/n$ is asymptotic. However the accuracy of the $k$th screening

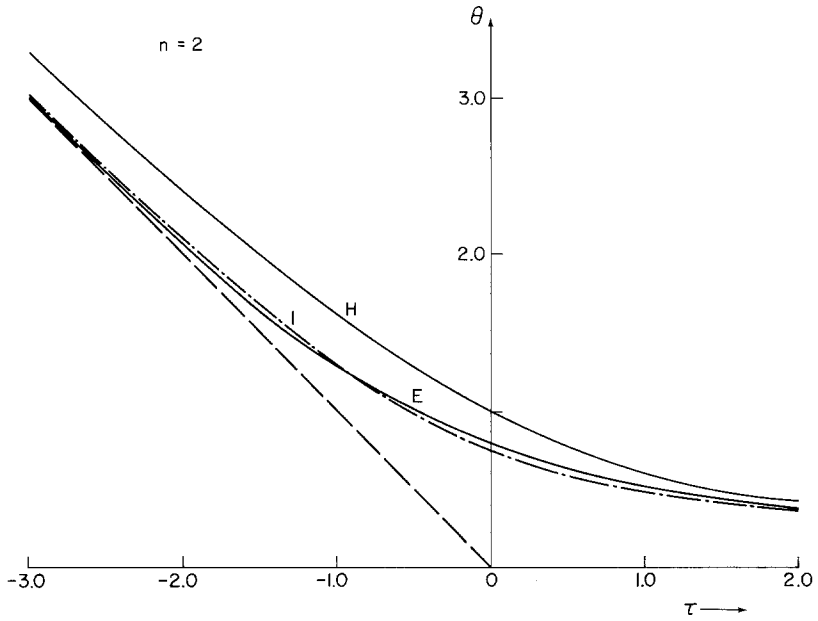


Fig. 1. Entropy function $\theta$ versus $\tau$ for $n = 2$. The exact, Hartree, and first screening solutions are labeled E, H, and 1, respectively. The dashed line through the origin represents mean field theory.

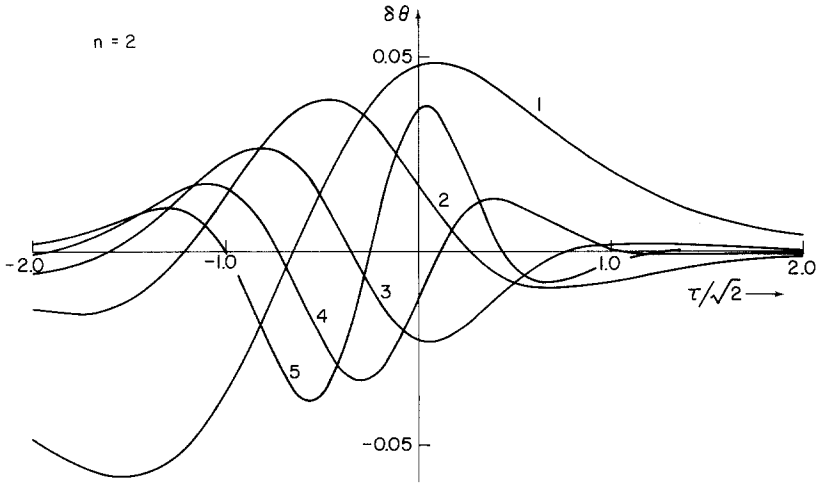


Fig. 2. Exact entropy function $\theta$ minus its value in the $k$th screening approximation, $\sum_{r=0}^{k} \theta_r \lambda^r$, plotted versus $\tau/\sqrt{2}$ for $n = 2$ ($\lambda = 1$). The first through the fifth screening approximations are labeled 1–5, respectively.

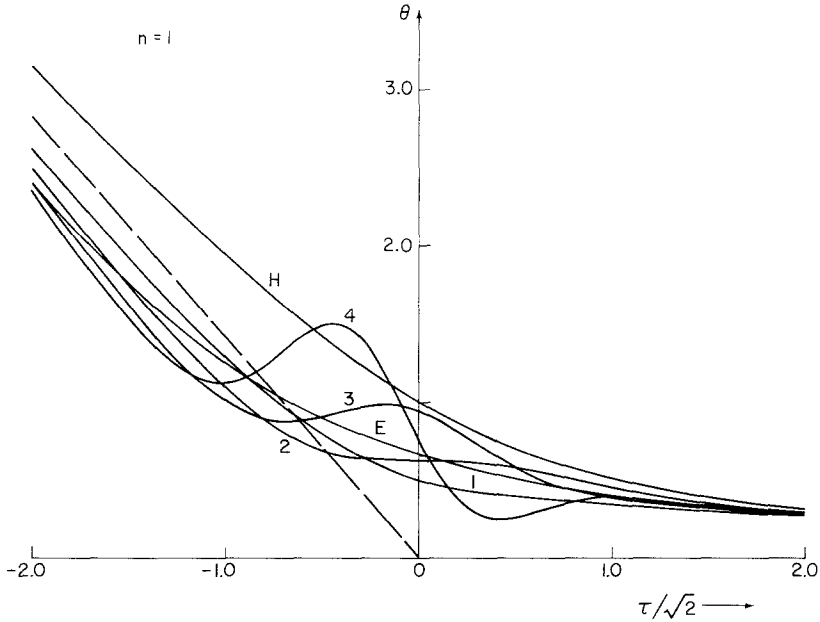


Fig. 3. Entropy function $\theta$ versus $\tau/\sqrt{2}$ for $n = 1$. Exact Hartree and first through fourth screening solutions are labeled E, H, and 1–4, respectively. The dashed line through the origin represents mean field theory.

approximation for small $k$ suggests that attempts to extend the approximation beyond $k = 2$ in one dimension and beyond $k = 1$ in two and three dimensions would be well worthwhile. This is one of the principal conclusions of this paper.

We turn now to the case $n = 1$ ($\lambda = 2$). Here the screening approximation deteriorates much more rapidly as $k$ increases. The results are plotted directly versus $\tau/\sqrt{2}$ in Fig. 3 for $k = 1$–4. Also plotted are the exact and Hartree solutions. Already for $k = 2$ the screening solution has a plateau region around $\tau = 0$, corresponding to a specific heat very near zero (the specific heat per component of the order parameter is $C = -\frac{1}{2}\, d\theta/d\tau$). For $k \geqslant 3$ wild oscillations set in. The result for $k = 5$ is not shown since the oscillations take the entropy function below zero. These results are further evidence of the asymptotic nature of the expansion.

## 4. THE SELF-CONSISTENT SCREENING APPROXIMATION

In the previous section we obtained approximate solutions to Eq. (11) by performing an expansion in powers of $\lambda = 2/n$, thus obtaining systematic corrections to the Hartree approximation. Inspection of the form of Eq. (11), however, suggests an approximation scheme which should give more accurate

results more quickly, namely an iteration of the first derivative term using the Hartree approximation as starting point. Recall the equation to be solved:

$$\theta^2 + \tau\theta = 1 + \lambda(d\theta/d\tau) \tag{17}$$

The Hartree approximation sets $\lambda = 0$, yielding

$$\theta^2 + \tau\theta = 1 \qquad \text{or} \qquad \tau = (1/\theta) - \theta$$

so that

$$d\theta/d\tau = -\theta^2/(1 + \theta^2) \tag{18}$$

The "first self-consistent screening approximation" is obtained by using Eq. (18) in Eq. (17) to give

$$\theta^2 + \tau\theta = 1 - [\lambda\theta^2/(1 + \theta^2)]$$

or

$$\alpha_1\theta^2 + \tau\theta = 1 \tag{19}$$

where

$$\alpha_1 = 1 + [\lambda/(1 + \theta^2)] \tag{20}$$

Equations (19) and (20) are amenable to simple numerical solution. Note that we have written $d\theta/d\tau$ as a function of $\theta$ in Eq. (18) rather than as a function of $\tau$. This increases the "self-consistency" of the approximation (we shall find in Section 5 that it corresponds in the graph-theoretic scheme to using fully dressed propagators everywhere). Further iterations are straightforward: Eqs. (19) and (20) are used to determine $d\theta/d\tau$ as a function of $\theta$; this function is then inserted into Eq. (17) to yield the next approximation for $\theta$. We refer to such subsequent approximations as the "second self-consistent screening approximation," and so on.

At this point we should remind the reader that Eq. (17) is of course exactly soluble in terms of the parabolic cylinder functions. The point of the present paper is to test the accuracy of well-defined approximation schemes which have been applied to the Ginzburg–Landau problem in higher dimensionalities. In Section 5 we shall find that the "self-consistent screening approximation" discussed here is identical in first iteration to the scheme used by Bray and Rickayzen[6,7] for calculating the specific heat in $d = 1$ and $d = 2$.

The $k$th self-consistent screening approximation produces an equation for $\theta$ of the form

$$\alpha_k\theta^2 + \theta\tau = 1 \tag{21}$$

giving

$$\frac{d\theta}{d\tau}\left(2\theta\alpha_k + \theta^2\frac{d\alpha_k}{d\theta} + \tau\right) + \theta = 0$$

or

$$\frac{d\theta}{d\tau} = \frac{-\theta^2}{1 + \theta^2[\alpha_k + \theta(d\alpha_k/d\theta)]} \tag{22}$$

A further iteration therefore yields a recursion relation for the $\alpha_k$:

$$\alpha_{k+1} = 1 + \frac{\lambda}{1 + \theta^2[\alpha_k + \theta(d\alpha_k/d\theta)]} \tag{23}$$

which, with the initial condition $\alpha_0 = 1$ appropriate to the Hartree approximation, generates all the self-consistent screening approximations. The first three $\alpha_k$ are given by

$$\begin{aligned}
\alpha_1 &= 1 + \frac{\lambda}{1 + \theta^2} \\
\alpha_2 &= 1 + \frac{\lambda(1 + \theta^2)^2}{1 + (3 + \lambda)\theta^2 + (3 - \lambda)\theta^4 + \theta^6} \\
\alpha_3 &= 1 + \lambda[1 + (3 + \lambda)\theta^2 + (3 - \lambda)\theta^4 + \theta^6]^2 \\
&\quad \times \{(1 + \theta^2)[1 + 3(2 + \lambda)\theta^2 + 3(5 + 2\lambda)\theta^4 + 4(5 + \lambda^2)\theta^6 \\
&\quad + 3(5 - 2\lambda)\theta^8 + 3(2 - \lambda)\theta^{10} + \theta^{12}]\}^{-1}
\end{aligned} \tag{24}$$

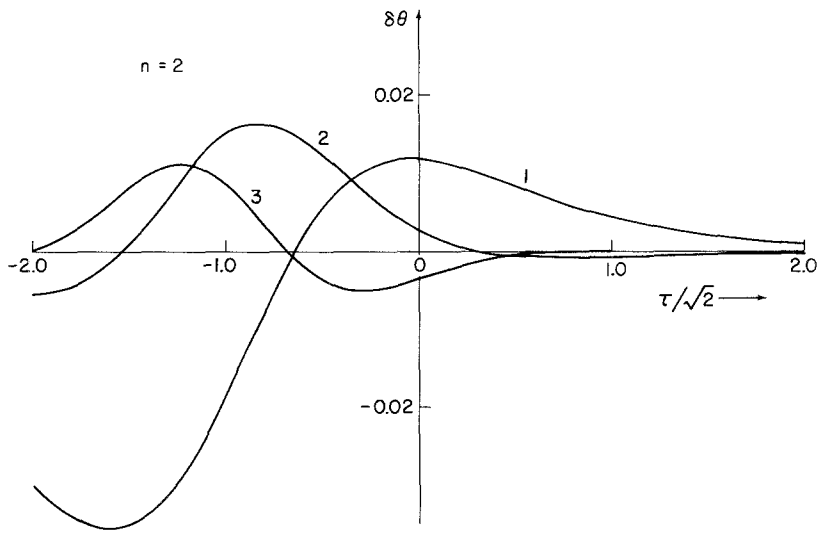


Fig. 4. Exact entropy function $\theta$ minus its value in the $k$th self-consistent screening approximation, $\theta^{(k)}$, versus $\tau/\sqrt{2}$ for $n = 2$. First through third self-consistent screening approximations are labeled 1–3, respectively. Note the change of vertical scale compared to Fig. 2.

For $n = 2$ ($\lambda = 1$) even the $k = 1$ result, $\theta^{(1)}$, is very close to the exact result $\theta$. The results are plotted as $\theta - \theta^{(k)}$ ($k = 1, 2, 3$) versus $\tau/\sqrt{2}$ in Fig. 4. The accuracy of these results is clearly substantially better than for the simple screening approximations of equivalent order discussed in Section 3. (Note the change of vertical scale compared to Fig. 2.) Furthermore, whereas the $1/n$ expansion ultimately diverges, it may be hoped that the self-consistent screening approximation will ultimately converge to the exact solution (though it is of course by no means certain to). On the debit side, the self-consistent screening approximation is more difficult to extend to higher dimensionalities than the $1/n$ expansion, particularly when results beyond the first iteration are desired (this will become clear in the following section). For $n = 1$ the iteration does not converge so rapidly. Results for $k = 1, 2, 3$ are plotted as $\theta^{(k)}$ versus $\tau/\sqrt{2}$ in Fig. 5.

## 5. GRAPH-THEORETIC CONSIDERATIONS

The theory of the Ginzburg–Landau model in terms of Feynman graphs is well known.[4–6] We are concerned in this section with a detailed application

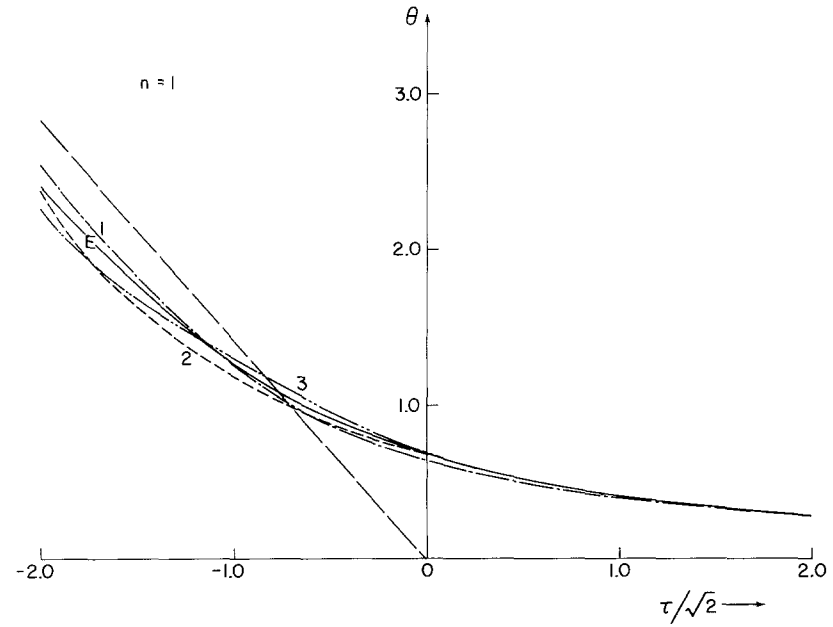


Fig. 5. Entropy function $\theta$ versus $\tau/\sqrt{2}$ for $n = 1$. Exact and first through third self-consistent screening solutions are labeled E and 1–3, respectively. The dashed line through the origin represents mean field theory.

of graph theory to the case $d = 0$. We begin by recalling Eq. (3) for the partition function:

$$Z = \int_{-\infty}^{\infty} \prod_{i=1}^{n} d\phi_i \exp\left[-\frac{1}{2}\tau \sum_{i=1}^{n} \phi_i^2 - \frac{1}{4n}\left(\sum_{i=1}^{n} \phi_i^2\right)^2\right] \tag{25}$$

This is the standard form of a $\phi^4$ field theory with the simplification for $d = 0$ that the "fields" $\phi_i$ have no spatial variation. We introduce the order parameter correlation function or "propagator" for the field $\phi_j$

$$\langle \phi_j^2 \rangle = \frac{1}{Z}\int_{-\infty}^{\infty} \prod_{i=1}^{n} (d\phi_i)\phi_j^2 \exp\left[-\frac{1}{2}\tau \sum_{i} \phi_i^2 - \frac{1}{4n}\left(\sum_{i} \phi_i^2\right)^2\right] \tag{26}$$

and note that is it simply equal to the entropy function $\theta\,[= -(2/n)\, d(\ln Z)/d\tau]$ since $\langle \phi_j^2 \rangle$ is independent of $j$. For $\tau \gg 1$ we can neglect the coupling between fields which is represented by the fourth-order terms in the exponents, to obtain the "bare" propagator:

$$\theta^0 = \langle \phi_j^2 \rangle^0 = 1/\tau \tag{27}$$

The "dressed" propagator $\theta$ is given by the usual graphical expansion[5,6] as the sum of all topologically distinct, linked graphs with two external lines. The graphs are evaluated according to the following rules:

1. Each bare propagator is represented by a solid line and associated with a factor $1/\tau$.
2. Each interaction vertex is represented by a dashed line with two solid lines joined to each end and is associated with a factor $-1/n$.
3. Each closed loop is associated with a factor $n$ (arising from a sum over components of the order parameter).
4. There is an overall factor $2^{l-m}$, where $l$ is the number of interaction vertices and $m$ the number of closed loops.

Consider a graph containing $l$ interaction vertices and $m$ closed loops. Then it must contain $2l + 1$ bare propagators and its value is given by the rules as

$$(1/\tau)^{2l+1}(-1/n)^l n^m 2^{l-m} = [(-1)^l/\tau^{2l+1}]\lambda^{l-m}, \qquad \text{where} \quad \lambda = 2/n \tag{28}$$

Hence an expansion in powers of $\lambda$ is derived by considering graphs with $l - m = 0, 1, 2, \ldots$. In zeroth order we require all graphs with equal numbers of interaction vertices and closed loops. This is the Hartree approximation and is shown in Fig. 6. A double bold line represents the dressed propagator $\theta_0$. Its use on the right-hand side in Fig. 6 enables us to sum the required infinite series of "bubble trees." Application of the rules gives

$$\theta_0 = (1/\tau) - (\theta_0^2/\tau)$$

or $\theta_0^2 + \tau\theta_0 = 1$, in agreement with Eq. (12).

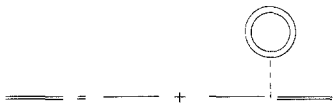

Fig. 6. Graphs for the entropy function $\theta$ within the Hartree approximation. Double solid lines represent dressed Hartree propagators and single solid lines represent bare propagators.

Terms of first order in $\lambda$ are given by graphs with one more interaction vertex than closed loop. All such graphs are generated by those of Fig. 7(a), where a wavy line represents the "screened potential"[6] and is defined by the graphical equation of Fig. 7(b). In Fig. 7 a single bold line now represents the Hartree propagator $\theta_0$. The screened potential is given by $(-1/n)v$, where application of the rules to Fig. 7(b) gives

$$v = 1/(1 + \theta_0^2) \tag{29}$$

As in Section 3, we seek an expansion of the form

$$\theta = \sum_{r=0}^{\infty} \theta_r \lambda^r \tag{30}$$

The graphs of Fig. 7(a) give

$$\theta_1 = v^2\theta_0^5 - v\theta_0^3 = -\theta_0^3/(1 + \theta_0^2)^2 \tag{31}$$

in agreement with Eq. (15).

With increasing order in $\lambda$ the number of graphs for $\theta$ increases extremely quickly. In second order, for example, there are 32. We give these in Fig. 8. The graphs are grouped in pairs labeled with unprimed and primed letters. In each case the primed graph is obtained from the unprimed graph by joining the external lines of the latter to form a closed loop which is connected by a wavy line to a new pair of external lines. (Note that the two diagrams of Fig. 7a are related in the same way; in fact, it is clear that graphs occur in such pairs to all orders in $\lambda$.) The value of a primed graph is related to that of its unprimed counterpart by a factor $-v\theta_0^2$, so that the two graphs together have a value $1 - v\theta_0^2 = v$ times the value of the unprimed graph. Henceforward, therefore, we will count only unprimed graphs and multiply by a

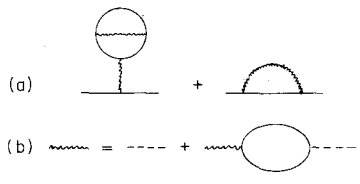


Fig. 7. (a) Order $\lambda$ corrections to the Hartree entropy. Solid lines represent Hartree propagators $\theta_0$ and wavy lines the screened potential $(-1/n)v$. (b) Graphical equation for the screened potential.

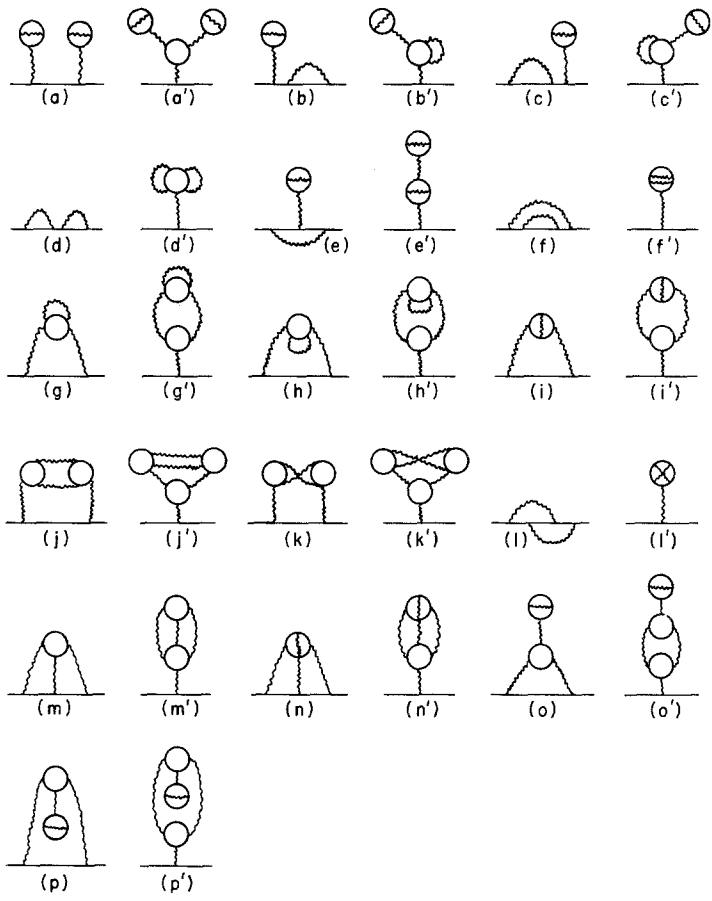


Fig. 8. Order $\lambda^2$ corrections to the Hartree entropy. Solid lines represent Hartree propagators $\theta_0$ and wavy lines the screened potential $(-1/n)v$.

factor $v$ to include the primed graphs. The unprimed graphs can be further grouped according to the number of wavy lines appearing. A graph (of order $\lambda^2$) with $l$ wavy lines has $2l + 1$ solid lines and $l - 2$ closed loops and therefore a value $(-v)^l\theta^{2l+1}\lambda^2$. Inspection of the unprimed graphs of Fig. 8 shows that there are three with $l = 2$, eight with $l = 3$, and five with $l = 4$. The total contribution to $\theta$ of all the graphs of Fig. 8 is therefore

$$v\lambda^2(3v^2\theta_0^5 - 8v^3\theta_0^7 + 5v^4\theta_0^9)$$

giving

$$\theta_2 = v^3\theta_0^5(3 - 8v\theta_0^2 + 5v^2\theta_0^4) = \theta_0^5(3 - 2\theta_0^2)/(1 + \theta_0^2)^5 \qquad (32)$$

in agreement with Eq. (15). The agreement is a check that we have indeed included all second-order graphs in Fig. 8. These same graphs give the order $\lambda^2$ contribution to $\theta$ for $d = 1$, 2, and 3, although, because of the spatial variation which enters, their evaluation is much more difficult than for $d = 0$. Our conclusions concerning primed and unprimed graphs still hold. The sum of such a pair is equal to $v(0)$ times the value of the unprimed graph, where $(-1/n)v(0)$ is the screened potential at zero momentum transfer. Further grouping of graphs is not helpful, however, since the value of a graph depends on its topological structure, in contrast to the case $d = 0$, when only the number of wavy lines is important.

The $1/n$ expansion can be performed more elegantly by considering the free energy function $F = -\ln Z$ rather than the entropy function $\theta$. This results in a considerable reduction in the number of graphs involved at the cost of a slight complexity in the counting of graphs. The details are given in Section 6.

We may consider the exact evaluation of $\theta$ by graphical means. This is of interest both as a rare example of the exact solution of a $\phi^4$ field problem by a graphical method and for the insight it gives into the nature of the self-consistent screening approximation. Now it is well known that the dressed propagator $\theta$ can be expressed in terms of a self-energy function $\sigma$ according to the graphs of Fig. 9(a) with $\sigma$ given exactly by the graphs of Fig. 9(b). Here a single bold line represents once more a bare propagator $1/\tau$, while a double bold line is the dressed propagator $\theta$. The shaded circle $\gamma$ is the fully renormalized three-point vertex and is given by an infinite graphical expansion, the first few terms of which are shown in Fig. 9(c). Figures 9(a) and 9(b) yield, respectively,

$$\theta = 1/(\tau + \sigma) \tag{33}$$

and

$$\sigma = \theta(1 + \lambda\gamma) \tag{34}$$

Now consider the expansion of $\sigma$ in terms of bare propagators. Differentiation with respect to $\tau$ has the effect of opening bare propagator lines in all possible ways so as to generate $\gamma$ via the relation

$$d\sigma/d\tau = \gamma - 1 \tag{35}$$

Equation (35) is the usual Ward identity relating the self-energy to the three-point vertex.

In one or more dimensions Eqs. (33)–(35) do not form a closed set, due to the momentum dependences which enter the problem. The vertex function depends on two momentum variables, $\gamma = \gamma(k, q)$, one of which (say $q$) is the momentum transferred at the vertex. The Ward identity, Eq. (35), only

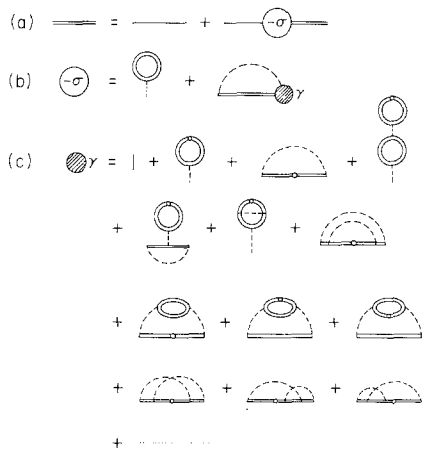


Fig. 9. (a) Relation between the dressed propagator $\theta$ and the self-energy $\sigma$. (b) Graphs giving the self-energy $\sigma$. (c) Graphical expansion for the three-point vertex $\gamma$. In all graphs double solid lines represent fully dressed propagators.

involves $\gamma(k, 0)$ since the operation of differentiating with respect to $\tau$ simply opens bare propagator lines without transferring any momentum. For $d = 0$, however, all momentum variables are zero (since the field $\phi_i$ has no spatial dependence) and simply drop out of the problem. Equations (33)–(35) then form a closed set. Equation (33) can be written

$$\sigma = 1/\theta - \tau \tag{36}$$

so that Eq. (35) becomes

$$\gamma = 1 + \frac{d\sigma}{d\tau} = -\frac{1}{\theta^2}\frac{d\theta}{d\tau} \tag{37}$$

Substituting into Eq. (34) then yields

$$1/\theta - \tau = \theta[1 - (\lambda/\theta^2)\, d\theta/d\tau]$$

or

$$\theta^2 + \theta\tau = 1 + \lambda\, d\theta/d\tau \tag{38}$$

This agrees with our exact result, Eq. (11).

We now turn to the self-consistent screening approximation in a graphical context. We see that this approximation consists simply in iterating Eq. (34) starting from $\gamma = 0$. Subsequent values of $\gamma$ are generated from Eq. (35) or, equivalently, Eq. (37). In fact we can substitute Eq. (37) into Eq. (38) to give

$$\theta^2 + \theta\tau = 1 - \lambda\gamma\theta^2$$

or

$$(1 + \lambda\gamma)\theta^2 + \theta\tau = 1 \tag{39}$$

Comparison of Eqs. (39) and (21) yields a simple relation between the $k$th iterated value of $\gamma$, $\gamma_k$, and the parameter $\alpha_k$ introduced in Section 4:

$$\alpha_k = 1 + \lambda\gamma_k \tag{40}$$

In order to obtain this equivalence, we require that $\gamma_k$ be written as a function of $\theta$ at each stage of the iteration rather than as a function of $\tau$. Graphically this clearly corresponds to using fully dressed propagators at each stage of the iteration. The graphical representation of the iteration procedure is shown in Fig. 10. In this form, of course, formal extension of the self-consistent screening approximation to higher dimensionalities is straightforward, though the equations represented by the graphs become extremely difficult to solve. Figure 10(c) gives the self-energy for the first self-consistent screening approximation which was used by Bray and Rickayzen[6,7] to calculate the specific heat for $d = 1$ and $d = 2$.

As a check that this graphical iteration is indeed identical to that of Section 4, we evaluate $\gamma_2$ from Fig. 10(d):

$$\begin{aligned}\gamma_2 &= 1 - \theta^2\gamma_2 - \lambda\theta^2 v\gamma_2 + 2\lambda\theta^4 v^2\gamma_2 \\ &= \left[1 + \theta^2 + \frac{\lambda\theta^2}{1 + \theta^2} - \frac{2\lambda\theta^4}{(1 + \theta^2)^2}\right]^{-1} \\ &= \frac{(1 + \theta^2)^2}{1 + (3 + \lambda)\theta^2 + (3 - \lambda)\theta^4 + \theta^6}\end{aligned} \tag{41}$$

in agreement with Eq. (24) via Eq. (40).

The graphical iteration procedure discussed here constitutes a method for extending beyond first order the self-consistent screening approximation of Bray and Rickayzen for arbitrary dimensionalities. We have seen in Section 4 that such a procedure may be expected to give more accurate results than a simple expansion in powers of $1/n$. However, for $d > 0$ the approximation takes the form of a set of nonlinear coupled integral equations which can only be solved by resorting to further approximations.[6,7] For $d = 2$, for example, the first-order set was solved by neglecting the momentum dependence of the self-energy.[7] Statements about the relative accuracy of the $1/n$ expansion and the thus approximated self-consistent screening method are difficult to make. In one dimension, however, for which exact results are known,[4,11] a simple approximation[6] of the set of equations for first-order self-consistent screening [based on expanding the self-energy $\sigma(q)$ as $\sigma(q) \sim a + bq^2$] yields results significantly better than those of the $1/n$ expansion in first or even second order.[3] We conclude that both the techniques discussed here merit further consideration for $d \geqslant 1$.

[3] Compare the results of Refs. 4 and 6.

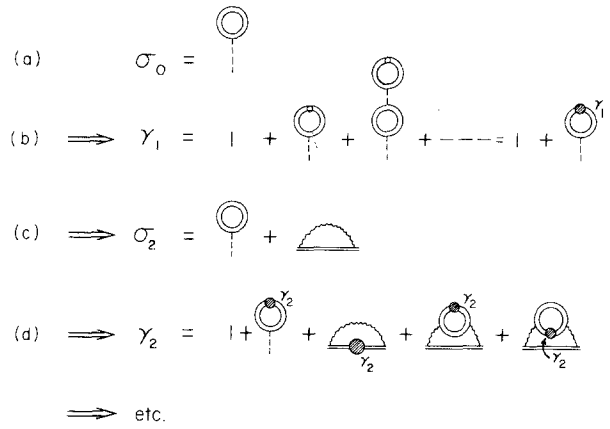


Fig. 10. Iteration procedure for the self-consistent screening approximation. At each stage of the iteration double solid lines represent dressed propagators to be determined self-consistently within the approximation at that stage.

## 6. GRAPHS FOR THE FREE ENERGY

In considering the $1/n$ expansion in Section 5 we noted that the number of graphs for the entropy function $\theta$ increases rapidly with increasing order in $1/n$, so that, for example, there are 32 graphs in order $1/n^2$. A considerable reduction in numbers can be obtained by constructing graphs for the free energy function $F$ defined by

$$F = -\ln Z \tag{42}$$

so that

$$\theta = \frac{2}{n}\frac{dF}{d\tau} = \lambda \frac{dF}{d\tau} \tag{43}$$

The graphs for $F$ are the usual topologically distinct, linked graphs with no external lines. They are evaluated according to rules 1–4 of Section 5 together with two extra rules:

5. There is an overall factor $(-1)$ corresponding to the minus sign in Eq. (42).
6. A graph with rotational symmetry $R$ is associated with an additional factor $1/R$.

The origin of rule 6 can be seen by considering Eq. (43). This shows that graphs for $\theta$ are derived from those for $F$ by opening bare propagator lines in all possible ways. An $F$ graph with rotational symmetry $R$ hence leads to $R$ identical $\theta$ graphs. Rule 6 may therefore be written more generally as,

"divide by the number of identical $\theta$ graphs produced on differentiation with respect to $\tau$."

To demonstrate the equivalence of the two expansions, we consider order $\lambda$ contributions to $F$ [leading via Eq. (43) to order $\lambda^2$ contributions to $\theta$]. These are graphs with one more wavy line than closed loop and are shown in Fig. 11. We make the derivation of rule 6 explicit by considering the correspondence of these graphs to those of Fig. 8 by means of Eq. (43). Recall that in both sets of graphs a single bold line represents a Hartree propagator $\theta_0$ and therefore contains all possible self-energy insertions of the Hartree type. Opening bare propagator lines in all possible ways, we find

11(a) → 8(d), (d'), (f), (f'), (g), (g'), (h), (h') (each in two ways)
11(b) → 8(i), (i'), (l), (l') (each in four ways)
11(c) → 8(a), (a'), (b), (b'), (c), (c'), (e), (e'), (o), (o'), (p), (p') (each in two ways)
11(d) → 8(m), (m'), (n), (n'), (j), (j'), (k), (k') (each in three ways)

Hence graphs 11(a), (b), (c), and (d) must be associated with factors $\frac{1}{2}$, $\frac{1}{4}$, $\frac{1}{2}$, and $\frac{1}{3}$, respectively, in agreement with rule 6, since the rotational symmetry factors are 2, 4, 2, and 3, respectively.

The evaluation of the graphs for $d = 0$ is simple. Application of the rules gives

$$F(\mathrm{a}) = -\tfrac{1}{2}\lambda v^2\theta_0{}^4, \qquad F(\mathrm{b}) = -\tfrac{1}{4}\lambda v^2\theta_0{}^4$$
$$F(\mathrm{c}) = \tfrac{1}{2}\lambda v^3\theta_0{}^6, \qquad F(\mathrm{d}) = \tfrac{1}{3}\lambda v^3\theta_0{}^6$$

The order $\lambda^2$ contribution to $\theta$ becomes, through Eq. (43),

$$\begin{aligned}\theta_2 &= \frac{d}{d\tau}\left(-\frac{3}{4}v^2\theta_0{}^4 + \frac{5}{6}v^3\theta_0{}^6\right)\\ &= -\frac{\theta_0{}^2}{1+\theta_0{}^2}\frac{d}{d\theta_0}\left(-\frac{3}{4}v^2\theta_0{}^4 + \frac{5}{6}v^3\theta_0{}^6\right)\\ &= \frac{\theta_0{}^2(3-2\theta_0{}^2)}{(1+\theta_0{}^2)^5}\end{aligned}$$

in agreement with Eq. (15).

As far as extensions to higher dimensionalities are concerned, it is clear

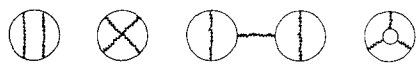


Fig. 11. Order $\lambda$ corrections to the Hartree free energy. Solid lines represent Hartree propagators $\theta_0$ and wavy lines the screened potential $(-1/n)v$.

that the free energy expansion is more convenient than the entropy expansion in view of the reduced numbers of graphs involved. Abe[12] has recently used the graphs of Fig. 11 to calculate order $1/n^2$ corrections to the critical exponent $\eta$ in three dimensions. The author has evaluated the same graphs for $d = 1$ and recovered the results of Ferrell and Scalapino,[4] obtained by a nongraphical method. Details will appear elsewhere.[13] The remaining and most difficult case, $d = 2$, is presently being studied.

In third- and higher-order screening approximations the number of graphs, even for the free energy, becomes large. We wish to emphasize the value of the case $d = 0$ for checking that all such graphs have been included. As an example, consider the graphs for third-order screening. Integration with respect to $\tau$ of the expression for $\theta_3$ given by Eq. (15) yields an expression for the free energy in third-order screening:

$$F_3 = \tfrac{5}{2}v^3\theta_0^6 - 10v^4\theta_0^8 + (25/2)v^5\theta_0^{10} - 5v^6\theta_0^{12} \tag{44}$$

Four classes of graph contribute to $F_3$: those with three wavy lines and one closed loop, those with four wavy lines and two closed loops, those with five wavy lines and three closed loops, and those with six wavy lines and four closed loops. Equation (44) tells us that the reciprocals of the rotational symmetry factors $R$ for graphs in the first class sum to $\frac{5}{2}$, for graphs in the second class to ten, in the third class to 25/2, and in the fourth class to five. Hence a study of the case $d = 0$ enables us to check graphs class by class. The graphs may then be evaluated in full confidence to obtain results in higher dimensionalities.

## 7. SUMMARY

We have used the exactly soluble zero-dimensional Ginzburg–Landau model to test the accuracy of two field-theoretic approximation schemes of current interest. These are the "screening approximation" of Ferrell and Scalapino, based on the $1/n$ expansion, and the "self-consistent screening approximation" of Bray and Rickayzen, based on an iteration of the coupled equations for the self-energy and the three-point vertex function. We have carried the former to fifth order and the latter to third order. For $n = 2$ the $1/n$ expansion seems to start diverging at the fifth-order term, whereas for $n = 1$ divergence sets in as early as the second-order term. The self-consistent screening approximation is more accurate for both $n = 2$ and $n = 1$ but is more difficult to extend to higher dimensionalities.

In conclusion we feel that efforts to extend the $1/n$ expansion beyond the present limits of second order for $d = 1$ and first order for $d = 2$ and $d = 3$ would be well worthwhile. Extension of the self-consistent screening approximation, though certainly more difficult, would perhaps prove even more

rewarding in terms of numerical accuracy. Where graphical methods are used the case $d = 0$ provides a simple method for checking that all relevant graphs have been included.

## ACKNOWLEDGMENTS

I would like to thank Prof. R. A. Ferrell for many helpful suggestions. I am indebted to the Fulbright–Hays Committee for a scholarship.

## REFERENCES

1. R. A. Ferrell and D. J. Scalapino, *Phys. Rev. Lett.* **29**:413 (1972); *Phys. Lett.* **41A**:37 (1972).
2. R. Abe, *Progr. Theor. Phys.* **48**:1414 (1972); S. K. Ma, *Phys. Rev. Lett.* **29**:1311 (1972).
3. D. J. Scalapino, R. A. Ferrell, and A. J. Bray, *Phys. Rev. Lett.* **31**: 292 (1973).
4. R. A. Ferrell and D. J. Scalapino, *Phys. Rev.* **A9**, 846 (1974).
5. A. J. Bray, Ph.D. Thesis, University of Kent at Canterbury (1973).
6. A. J. Bray and G. Rickayzen, *J. Phys. F.: Metal Phys.* **2**:L109 (1972).
7. G. Rickayzen and A. J. Bray, *J. Phys. F.: Metal Phys.* **3**:L134 (1973).
8. R. Balian and G. Toulouse, *Ann. of Phys.* **83**, 28 (1974).
9. B. Muhlschlegel, D. J. Scalapino, and R. Denton, *Phys. Rev. B* **6**:1767 (1972).
10. M. Abramowitz and I. A. Stegun, *Handbook of Mathematical Functions*, National Bureau of Standards, Chapter 19.
11. D. J. Scalapino, M. Sears, and R. A. Ferrell, *Phys. Rev. B* **6**:3409 (1972).
12. R. Abe, *Progr. Theor. Phys.* **49**:1877 (1973).
13. A. J. Bray, "Statistical Mechanics of One-Dimensional Ginzburg–Landau Fields: Feynman Graph Evaluation of the Screening Approximate ($n^{-1}$ Expansion)," University of Maryland Technical Report No. 74-049 (1973).